

OVER 5000 DISTANT EARLY-TYPE GALAXIES IN COMBO-17:
A RED SEQUENCE AND ITS EVOLUTION SINCE $Z \sim 1$

ERIC F. BELL¹, CHRIS WOLF², KLAUS MEISENHEIMER¹, HANS-WALTER RIX¹, ANDREA BORCH¹, SIMON DYE³, MARTINA KLEINHEINRICH⁴, AND DANIEL H. MCINTOSH⁵

¹ Max Planck Institut für Astronomie, Königstuhl 17, D-69117 Heidelberg, Germany;
bell,meise,rix,borch@mpia.de

² Department of Physics, Denys Wilkinson Bldg., University of Oxford, Keble Road, Oxford, OX1 3RH, UK;
cwolf@astro.ox.ac.uk

³ Astrophysics Group, Blackett Laboratory, Imperial College, Prince Consort Road, London SW7 2BW, UK;
s.dye01@imperial.ac.uk

⁴ IAEF, Universität Bonn, Auf dem Hügel 71, D-53121, Bonn, Germany; martina@astro.uni-bonn.de

⁵ Department of Astronomy, University of Massachusetts, 710 North Pleasant Street, Amherst, MA 01003-9305;
dmac@hamerkop.astro.umass.edu

SUBMITTED TO THE ASTROPHYSICAL JOURNAL: *March 17, 2003*

ABSTRACT

We present the rest-frame colors and luminosities of $\sim 25000 m_R \lesssim 24$ galaxies in the redshift range $0.2 < z \leq 1.1$, drawn from 0.78 square degrees of the COMBO-17 survey. We find that the rest-frame color distribution of these galaxies is bimodal at all redshifts out to $z \sim 1$. This bimodality permits a model-independent definition of red, early-type galaxies and blue, late-type galaxies at any given redshift. The colors of the blue peak do not change with redshift; however, the number density of blue luminous galaxies has dropped strongly since $z \sim 1$. Red galaxies populate a color-magnitude relation. Such red sequences have been identified in galaxy cluster environments, but our data show that such a sequence exists over this redshift range even when averaging over all environments. The mean color of the red galaxy sequence evolves with redshift in a way that is consistent with the aging of an ancient stellar population. The rest-frame *B*-band luminosity density in red galaxies evolves only mildly with redshift in a Λ -dominated cold dark matter Universe. Accounting for the change in stellar mass-to-light ratio implied by the redshift evolution in red galaxy colors, the COMBO-17 data indicate an increase in stellar mass on the red sequence by a factor of two since $z \sim 1$. The largest source of uncertainty is large-scale structure, implying that considerably larger surveys are necessary to further refine this result. We explore mechanisms that may drive this evolution in the red galaxy population, finding that both galaxy merging and truncation of star formation in some fraction of the blue, star-forming population are required to fully explain the properties of these galaxies.

Subject headings: galaxies: evolution — galaxies: general — galaxies: luminosity function — galaxies: elliptical and lenticular — galaxies: stellar content — surveys

1. INTRODUCTION

The evolution of early-type galaxies since early in the Universe's history is a highly active area of research. The current world model for the evolution of the Universe is the Cold Dark Matter paradigm; the incarnation which appears consistent with most observations adopts $\Omega_m = 0.3$, $\Omega_\Lambda = 0.7$, and $H_0 = 100 h \text{ km s}^{-1} \text{ Mpc}^{-1}$, where $h \sim 0.7$ (the Λ CDM paradigm; e.g., Freedman et al. 2001; Efstathiou et al. 2002; Pryke et al. 2002; Spergel et al. 2003). In this model, early-type galaxies form hierarchically through mergers of pre-existing galaxies (e.g., White & Frenk 1991; Barnes 1992; Cole et al. 2000). A generic prediction of this type of model is an increase in the stellar mass density of the early-type galaxy population since $z \sim 1$, as large galaxies are assembled primarily at relatively late times (e.g., Aragon-Salamanca, Baugh, & Kauffmann 1998; Kauffmann & Charlot 1998). Therefore, an important test of the hierarchical formation scenario is to quantify the evolution of early-type galaxies since $z \sim 1$. In this paper, we discuss the color distributions of a sample of ~ 25000 galaxies from the COMBO-17 survey ('Classifying Objects by Medium-Band Observations in 17 Filters'; Wolf et al. 2003), focusing on an objective definition of early-type galaxies at all redshifts. We then use this objectively-defined sample of early-type galaxies with $0.2 < z \leq 1.1$ to examine the evidence for a substantial build-up of stellar mass in red galaxies since $z \sim 1$.

In the local Universe, early-type galaxies have historically been defined in terms of morphology. Loosely speaking, galaxies with dominant smooth spheroidal components, and at most a modest and smooth disk, will be classified as an 'early-type' galaxy. These galaxies tend to be red in optical color both locally (e.g., Schweizer & Seitzer 1992) and out to $z \sim 1$ (e.g., Kodama, Bower, & Bell 1999). This definition of early-type galaxies is being challenged by the recent demonstration that galaxies are distributed in color space in a bimodal distribution (see, e.g., Strateva et al. 2001; Hogg et al. 2002; Blanton et al. 2003a). One peak is red, and consists mostly of non-star-forming galaxies earlier than *Sa* in morphological type. The other peak is blue and consists primarily of star-forming galaxies later than *Sb* in morphological type (Strateva et al. 2001). Because of this bimodality in color and therefore star formation history (SFH), it is defensible, and perhaps more natural, to define early types in terms of colors (i.e., spectral energy distribution or SFH). These different definitions seem largely consistent (e.g., Schweizer & Seitzer 1992; Strateva et al. 2001; Bell et al. 2003). In this paper, we split the galaxy population into red and blue subsets based on their rest-frame optical colors, exploring the evolution of these populations with cosmic time.

In the local Universe, the blue-peak galaxies (later types) show a scattered but systematic variation of color with magnitude, in the sense that luminous galaxies tend to be some-

what less blue (e.g., Tully et al. 1998; Hogg et al. 2002). These color changes, when examined in detail, are due to changes in the mean ages, metallicities, and dust contents of galaxies with galaxy magnitude, such that brighter galaxies tend to be older, dustier, and more metal-rich (see, e.g., Tully et al. 1998; Bell & de Jong 2000). In contrast, red-peak galaxies (earlier types) have a tighter and well-defined relationship between color and magnitude, such that bright galaxies are typically redder (e.g., Sandage & Visvanathan 1978; Bower, Lucey, & Ellis 1992; Schweizer & Seitzer 1992; Terlevich, Caldwell, & Bower 2001). This color-magnitude relation (CMR) is well-established in overdense and cluster environments, where early-type galaxies are much more common (Dressler 1980; Dressler et al. 1997). Nevertheless, the CMR also exists among present-day field early-type galaxies (e.g., Sandage & Visvanathan 1978; Schweizer & Seitzer 1992; Hogg et al. 2003). The scatter, slope and evolution of the CMR in clusters of galaxies are all consistent with the interpretation of the CMR as primarily a metallicity sequence of old galaxies, where more massive galaxies are more metal-rich (e.g., Bower, Lucey, & Ellis 1992; Kodama & Arimoto 1997; Vazdekis et al. 2001; Bernardi et al. 2003). A modest age spread is possible (Trager et al. 2000).

The evolution of the properties of individual early-type galaxies with redshift has been studied in clusters of galaxies, where the assembly of sizeable galaxy samples has been feasible. It appears as if individual early-type galaxies were formed relatively quickly at high redshift and simply aged to the present day through so-called passive evolution (e.g., Kodama & Arimoto 1997; Kelson et al. 2001; van Dokkum et al. 2003). This has been used to justify ‘monolithic collapse’ models of early-type galaxy formation, where these galaxies form quickly early in the history of the Universe, and simply age to the present day (e.g., Eggen, Lynden-Bell, & Sandage 1962; Larson 1975; Kodama & Arimoto 1997; Nulsen & Fabian 1997). Yet, monolithic collapse, at best, is mildly unphysical; the hierarchical build-up of galaxies through mergers and interactions must happen at some level (e.g. White & Frenk 1991).

An elegant interpretation of the apparent contradiction between seemingly passive evolution and the hierarchical build-up of early-type galaxies has been put forward by van Dokkum & Franx (2001, progenitor bias). They note that studies of the properties of early-type galaxies in isolation (rightfully) fail to study the star-forming precursors of galaxies that are later destined to become early types. Thus, individual early-type galaxies appear old at all redshifts regardless of whether they were formed in a burst at redshift infinity or whether their formation happens through violent mergers which consume all of the gas in the interacting galaxies, leaving a spheroidal remnant (e.g., Toomre & Toomre 1972; Barnes & Hernquist 1996). This is a common theme in many contemporary studies of early-type galaxies; the distinction between when the *stars* in early-type galaxies were formed, and when the *galaxies* were assembled into recognizable entities. Studies of galaxies selected by strong gravitational lensing largely avoid this bias by selecting by mass (e.g., Kochanek et al. 2000; Rusin et al. 2003; van de Ven, van Dokkum, & Franx 2003); yet, these studies also find rather ancient-looking stellar populations.

Thus, a more important constraint on the evolution of early-type galaxies — and therefore, a stronger test of galaxy formation models — is the evolution of their number density and luminosity function (whether the early-type galaxy population is defined by morphology or color). Here, the situation is some-

what less clear. Many studies find that the evolution of the early-type population is close to passive up to $z \sim 1$, with perhaps a slight decrease in number density above $z \sim 1$ (e.g., Lilly et al. 1995; Schade et al. 1999; Lin et al. 1999; Cimatti et al. 2002; Firth et al. 2002; Im et al. 2002; Chen et al. 2003; Pozzetti et al. 2003). Other studies find relatively rapid evolution. For example, Kauffmann et al. (1996) find number evolution of a factor of three by $z \sim 1$, although Totani & Yoshii (1998) argue that spectroscopic incompleteness causes this apparent evolution, and state that Kauffmann et al.’s results are consistent with passive evolution. Wolf et al. (2003) find a rapid increase in the luminosity density of galaxies with the colors of *present-day* early-type galaxies from $z \sim 1$ until the present day; yet, passive evolution and reddening of the galaxy population is likely responsible for much of this.

Nevertheless, a problem shared by most surveys of early-type galaxies at $z \gtrsim 0.5$ has been susceptibility to large scale structure. Surveys to date have typically had samples of only 50–1500 early-type galaxies (e.g., Kauffmann & Charlot 1998; Schade et al. 1999; Lin et al. 1999; Firth et al. 2002; Chen et al. 2003; Pozzetti et al. 2003). Furthermore, these samples are usually from relatively small areas on the sky (the largest are CNOC2 and the LCIRS with 1400 square arcminutes each; Lin et al. 1999; Chen et al. 2003). Worse still, early-type galaxies are strongly clustered (e.g., Dressler 1980; Dressler et al. 1997; Moustakas & Somerville 2002; Daddi et al. 2002), which means that the measured number evolution is particularly sensitive to large-scale structure. Thus, to accurately measure the evolution of the stellar mass in early-type galaxies, it is necessary to use as large an area on the sky as possible.

In this paper, we bring the largest present-day sample of galaxies with $0.2 < z \leq 1.1$ to bear on this important problem. The COMBO-17 survey has to date imaged and fully analyzed three ~ 0.25 square degree fields in 5 broad-band and 12 narrow-band filters (data for a fourth field has been taken but is not yet analyzed). The 5 broad and 12 narrow-bands allow the construction of photometric redshifts and rest-frame colors with extraordinary precision (one can think of the data as a $R \sim 10$ ultra-low resolution spectrum rather as a photometric dataset), yielding galaxy redshifts accurate to a few percent for a total sample of ~ 25000 galaxies in 0.78 square degrees (2800 square arcminutes) with $m_R < 24$. We use this sample to discuss the colors of galaxies with $0.2 < z \leq 1.1$, focusing particularly on the reddest galaxies at all redshifts. We put forward an objective definition of early-type galaxies, and use this definition to explore the evolution of the red galaxy population from redshift unity to the present day.

This paper is set out as follows. The COMBO-17 survey and the main sources of error are briefly discussed in §2. In §3, we explore the colors of the entire COMBO-17 galaxy population with $0.2 < z \leq 1.1$. Then, in §4, we focus on the reddest galaxies at all redshifts, exploring their CMR in more detail. Defining early-type galaxies as galaxies on the CMR, we then go on in §5 to explore the evolution of the luminosity function of red galaxies. We discuss the results in §6, and present the conclusions in §7. Throughout, we assume $\Omega_m = 0.3$, $\Omega_\Lambda = 0.7$, and $H_0 = 100 h \text{ km s}^{-1} \text{ Mpc}^{-1}$. In order to estimate the passive evolution of stellar populations as a function of lookback time, we adopt $h = 0.7$ to be consistent with the *Hubble Space Telescope* Key Project distance scale (Freedman et al. 2001) and the recent results from the *Wilkinson Microwave Anisotropy Probe* (Spergel et al. 2003).

2. THE DATA

The COMBO-17 data, the sample selection, redshift estimation, construction of rest-frame luminosities, and completeness are all discussed in detail by Wolf et al. (2003, W03 hereafter), Wolf et al. (2001a, W01 hereafter), Wolf et al. (2001b), and in a forthcoming technical paper (Wolf et al., in preparation). Here, we briefly discuss the relevant limitations and sources of uncertainty in the COMBO-17 data.

2.1. Data and Sample Selection

To date, the COMBO-17 project has surveyed 0.78 square degrees to deep limits in three pointings (see Table 1) of the Wide Field Imager (WFI; Baade et al. 1998, 1999) at the Max Planck Gesellschaft/European Southern Observatory 2.2-m telescope at La Silla, Chile. The WFI has eight $2k \times 4k$ CCDs, a field of view of $34' \times 33'$, and a pixel scale of $0''.238/\text{pixel}$. A total of $\sim 160k$ sec per field were taken in 5 wide and 12 medium passbands with $3640\text{\AA} \leq \lambda_{\text{obs}} \leq 9140\text{\AA}$; an ultra-deep 20ksec R -band with seeing below $0''.8$ and a 10σ limiting magnitude of 25.2, and deep $UBVI$ and 12 medium passbands designed to allow the construction of low-resolution $R \sim 10$ spectra, or equivalently accurate photometric redshift estimates, for a total of ~ 25000 objects with $0.2 \leq z \leq 1.2$. The comoving survey volume is $\sim 10^6 h^{-3} \text{Mpc}^3$ in the interval $0.2 < z \leq 1.1$, split between three disjoint roughly equally-sized fields.

Galaxies were detected in the deep R -band frames using SExtractor (Bertin & Arnouts 1996), and we adopt the MAG-AUTO magnitude as our total magnitude estimate (a Kron 1980, magnitude in uncrowded regions). Bertin & Arnouts (1996) show that this magnitude underestimates the flux in galaxies by $\sim 6\%$. We do not correct for this effect as almost all local galaxy surveys adopt similarly biased Kron or Petrosian magnitudes (e.g., Blanton et al. 2003b; Skrutskie et al. 1997). The spectral shapes for R -band detected objects were measured by performing seeing-adaptive, weighted aperture photometry in all 17 frames at the position of the R -band detected object using the package MPIAPHOT (Röser & Meisenheimer 1991, Meisenheimer et al., in preparation). This package measures the peak surface brightness of all of the images smoothed to identical seeing ($\sim 1''.5$) to maximize signal-to-noise. Thus, the colors are essentially total for distant objects and are central colors for more extended, nearby galaxies. Photometric calibration was achieved using spectrophotometric standards in each COMBO-17 field. All magnitudes are quoted in Vega-normalized magnitudes. The median galaxy in our sample with $m_R \sim 22$ has observed galaxy magnitude errors of $\delta_R \sim 0.01$ mag, $\delta_{B,V,I} \sim 0.05$

TABLE 1
COMBO-17 FIELDS

Field	RA J2000.0	Dec J2000.0	l	b	$E(B-V)$
CDFS	03 ^h 32 ^m 25 ^s	-27°48'50"	223°6	-24°5	0.01
A 901	09 ^h 56 ^m 17 ^s	-10°01'25"	248°0	+33°6	0.06
S11	11 ^h 42 ^m 58 ^s	-01°42'50"	270°5	+56°8	0.02

Note. — $E(B-V)$ is estimated following Schlegel, Finkbeiner, & Davis (1998)

mag, $\delta_U \sim 0.3$ mag, and δ_{Medium} for the medium passbands increasing from 0.03 mag at the red end to 0.2 mag at the blue end.

2.2. Photometric Redshifts, Spectral Templates and Rest-Frame Colors

The full survey dataset is photometrically classified into stars, galaxies and AGN using the 17-passband ‘fuzzy’ spectrum (W01). No attempt is made to use morphological information, as, for example, double stars may contaminate the galaxy catalog, and compact galaxies may contaminate the stellar or AGN catalogs. For galaxy classification, we use PÉGASE (see Fioç & Rocca-Volmerange 1997, for an earlier version of the model) model spectra which have been tuned to fit the Kinney et al. (1996) template spectra. These spectra are defined in the interval $1216\text{\AA} \leq \lambda_{\text{obs}} \lesssim 10000\text{\AA}$ for elliptical through to starburst galaxies. We have applied an empirical adjustment to the near-UV spectral region of early-type galaxy templates to better reproduce the spectroscopic redshifts of galaxies in the Abell 901 cluster and other galaxies in the Chandra Deep Field South with $z \lesssim 1$. Trustworthy templates shortwards of 1216\AA have not yet been included, limiting redshift measurements at this stage to $z < 1.55$. For our subsequent analysis the redshift range is further limited to $z \leq 1.1$ in order to have at least two filters redwards of the 4000\AA break. The template library does not evolve, and does not include spectral types which are unusual in the local Universe, most notably for our purposes, dusty starbursting galaxies and post-starburst E+A galaxies. For galaxies and AGN, galaxy redshifts are estimated simultaneously with the template type (W01). A description of an earlier version of this methodology was presented by W03, and a full description and analysis of these photometric redshifts and classifications will be presented by Wolf et al. (in preparation) and Borch et al. (in preparation).

The galaxy redshift estimation quality has not yet been thoroughly tested for COMBO-17. Tests with a very similar multi-color survey (the ‘Calar-Alto Deep Imaging Survey’; CADIS) indicate that the redshift quality for early-type galaxies with strong 4000\AA breaks in COMBO-17 will be better than the mean CADIS redshift accuracy of $\delta z \sim 0.03$. For star-forming and starbursting later types, the accuracy is lower $\delta z \lesssim 0.1$ owing to the lack of a strong 4000\AA break. Restframe colors and luminosities are constructed on a galaxy-by-galaxy basis by k -correcting the nearest observed broad band flux. To estimate this k -correction, we convolve the best-fit spectrum with the filter curves for the Johnson U , B , and V passbands. Typical rest-frame color accuracy is ~ 0.1 mag, corresponding to the redshift uncertainty $\Delta z \sim 0.03$. Absolute magnitudes have an additional error of ~ 0.1 mag ($z \gtrsim 0.5$) and ~ 0.3 mag ($z \sim 0.3$) owing to distance uncertainties. See Wolf et al. (2001b) for more details.

2.3. Completeness

We include only galaxies with successful photometric redshift and spectral classifications. Therefore, when constructing luminosity functions and densities, we must account for the sample completeness. This is done using extensive Monte-Carlo simulations of the galaxy detection, photometry and classification process (W01); example completeness maps are shown in Fig. 7 of W03. For the red galaxies which are the primary aim of this paper, the 90% and 50% completeness limits are at roughly $m_R \sim 23.2$ and ~ 23.8 , respectively.

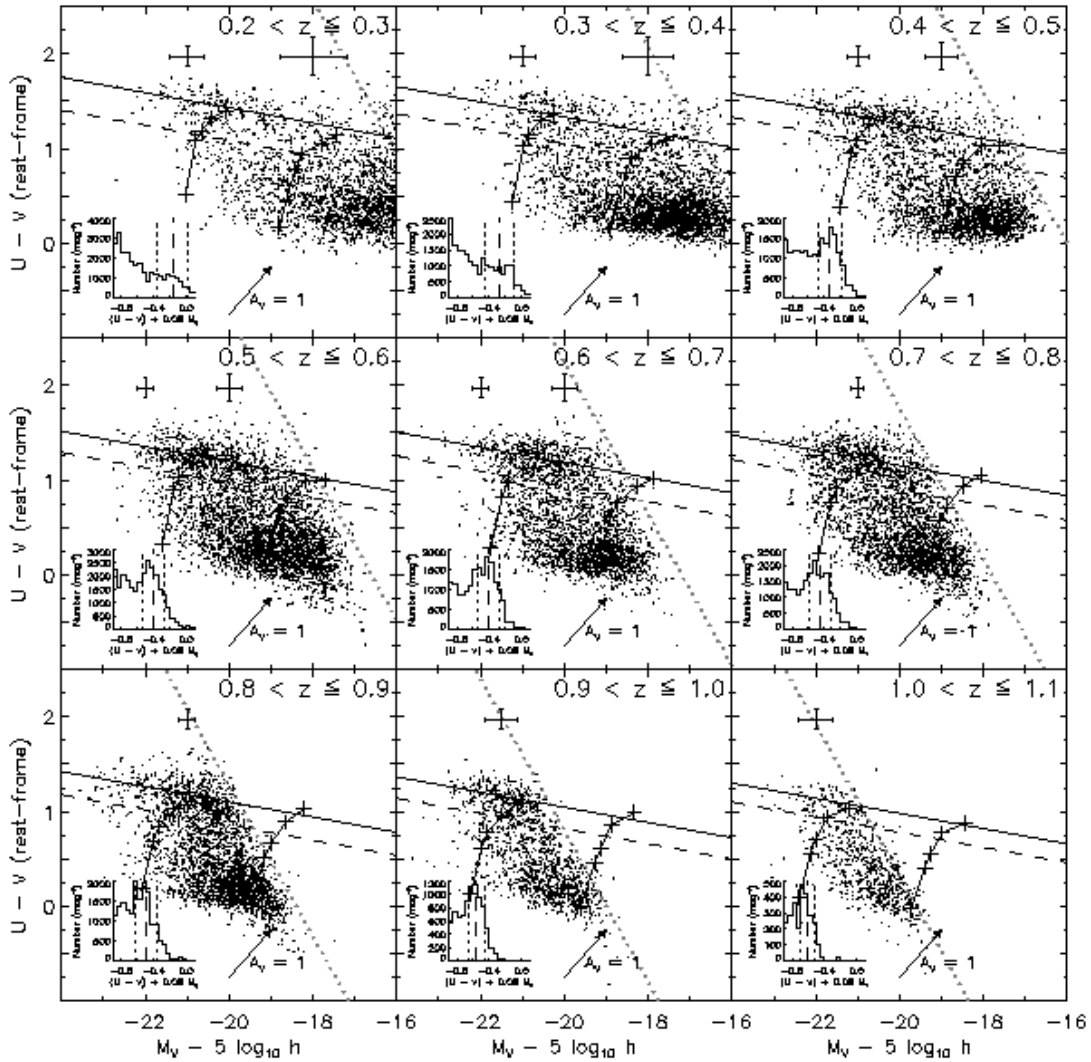


FIG. 1.— The rest-frame $U-V$ color of ~ 25000 galaxies against the absolute magnitude in V -band, $M_V - 5 \log_{10} h$. We show the distribution of galaxies in nine different redshift bins. A fit to the color-magnitude relation of red-sequence galaxies with a fixed slope of -0.08 is shown by the solid line, and the ‘Butcher-Oemler’ style-cut between red and blue galaxies is shown by the dashed line parallel to the early-type galaxy CMR (see §5). The sloping cutoff in the distribution of galaxies at the faint end (denoted roughly by the grey dotted line) is due to the $m_R \lesssim 24$ magnitude limit of the survey. The lines with crosses show the colors and magnitudes of model galaxies with truncated SFHs with constant stellar mass, described in more detail in §6.4. Representative error bars are shown. For reference, we show a reddening vector from Calzetti et al. (2000) assuming $A_V = 1$ mag; a Milky-Way extinction curve gives the same vector. Shown in the inset panels is the color distribution of the red peak at each redshift (with the slope of the CMR taken out); the dashed line indicates the position of the biweight mean that we adopt as the CMR ridge-line, and the dotted lines show the biweight sigma that we adopt as the CMR red sequence’s scatter.

3. THE COLOR DISTRIBUTION OF GALAXIES WITH $0.2 < z \leq 1.1$

One of the main aims of this paper is to explore and discuss the color distribution of galaxies in the interval $0.2 < z \leq 1.1$. We choose to quantify this in terms of $U-V$ color as a function of V -band absolute magnitude, because the $U-V$ color straddles the 4000\AA break and is therefore particularly sensitive to age and metallicity variations of the stellar populations in galaxies, and for consistency with well-known works from the literature (e.g., Sandage & Visvanathan 1978; Bower, Lucey, & Ellis 1992; Schweizer & Seitzer 1992). In Fig. 1, we show the distribution of rest-frame $U-V$ galaxy color against the V -band absolute magnitude in nine different redshift bins covering $0.2 < z \leq 1.1$.

Fig. 1 shows one of the key observational results of this paper, that the distribution of galaxies in the color-magnitude diagram is strikingly bimodal at all redshifts out to $z \sim 1$. This

confirms and extends nearly 10 Gyr back in time the *Sloan Digital Sky Survey* (SDSS) results from e.g., Strateva et al. (2001), Hogg et al. (2002), or Blanton et al. (2003a), who established and characterized the bimodality of the color distribution of galaxies in the local Universe. Furthermore, this confirms the suggestion of Im et al. (2002), who saw hints of a bimodal color distribution out to $z \sim 1$.¹ For immediate low-redshift comparison, we show a synthesized $U-V$ color-magnitude diagram for galaxies from the SDSS Early Data Release in the Appendix. This brings up a number of interesting questions. For example, does this bimodality mean that galaxies with $z \lesssim 1$ are either forming stars rapidly (the blue peak) or hardly at all (the red peak)? Put differently, is there a bimodal distribution of specific star formation rates? Or, does this bimodality simply tell us that if any star formation happens at all it dominates the opti-

¹The DEEP2 survey with Keck also appears to find this bimodality (B. Weiner, 2003, priv. comm.)

cal colors? A full stellar populations analysis is clearly merited, but is beyond the scope of this paper. We do, nevertheless, return to this issue briefly in §6.5.

Beyond the bimodality, it is important to notice two features of Fig. 1. Firstly, the rest-frame $U - V$ colors of blue galaxies do not significantly evolve with redshift. However, their number density, especially at high luminosities, significantly evolves. Luminous blue galaxies are *much* less common today than they were at redshift one (e.g., Cowie et al. 1996). This is consistent with Fig. 16 of W03; while the number density of faint star-forming galaxies (spectral Type 4) remains almost unchanged, the abundance of luminous galaxies with starburst spectra drops precipitously from redshift unity to the present epoch. This result, which is discussed much more by W03, also agrees with the CNOC2 (Lin et al. 1999) and CFRS (Lilly et al. 1995) surveys, who found strong evolution in the abundance of star-forming, blue galaxies with redshift.

Secondly, the red galaxies form a relatively well-defined sequence in the color-magnitude plane for $0.2 < z \leq 1.1$. Furthermore, the mean color of this red sequence evolves with redshift, in the sense that galaxies become bluer at a fixed luminosity. This evolution will be quantified in §4. Both observations agree with studies of galaxies in clusters at redshifts up to unity (e.g., Bower, Lucey, & Ellis 1992; Kodama & Arimoto 1997; Terlevich, Caldwell, & Bower 2001; van Dokkum & Franx 2001), but we extend these results by showing that they apply to volumes which average over many different environments. The red sequence has a significant slope in the color-magnitude plane, therefore can be rightfully termed a color-magnitude relation (CMR) in all redshift bins up to at least $z \sim 0.8$. At $z \gtrsim 0.8$, the magnitude range is so narrow that a constant color is also quite plausible. It is the CMR of the red sequence galaxies that we study in detail in the rest of this paper.

4. THE COLOR-MAGNITUDE RELATION OF RED GALAXIES

We now quantify the redshift evolution of the CMR by examining its zero point. In order to ensure consistency between the zero point estimates for different bins, we constrain the slope of the CMR to the locally-determined value $d(U - V)/dM_V = -0.08$ (Bower, Lucey, & Ellis 1992; Terlevich, Caldwell, & Bower 2001). We determine the robust biweight mean color, with the locally-determined CMR slope subtracted, of all galaxies with $U - V > 1.0$ (independent of redshift, so as to roughly isolate the red sequence). We illustrate the procedure by showing the CMR-subtracted color histogram of galaxies in the inset panels. The biweight mean and sigma are denoted by the dashed and dotted lines respectively. It becomes clear that the peak of the distribution can be determined to within a few hundredths of a magnitude, which is sufficient for our purposes.

The value of this fit to the CMR at $M_V - 5 \log_{10} h = -20$ is shown as a function of redshift in Fig. 2. It is clear that this population evolves considerably between $z = 1.1$ and 0.2; the galaxies become redder by ~ 0.4 mag. The biweight RMS for the red sequence is given by the error bar. Overplotted are the evolving $U - V$ colors expected for single-age populations with differing formation redshifts. We use the PÉGAUSE stellar population synthesis model with subsolar metallicities to predict colors at a constant absolute magnitude. Galaxies with $M_V - 5 \log_{10} h = -20$ at redshift zero would be brighter at redshift one, owing to passive evolution of the stellar population. Therefore, we apply a small color correction to account for the fact that the galaxies with $M_V - 5 \log_{10} h = -20$ at redshift one are from a different, bluer part of the CMR. The evolution of

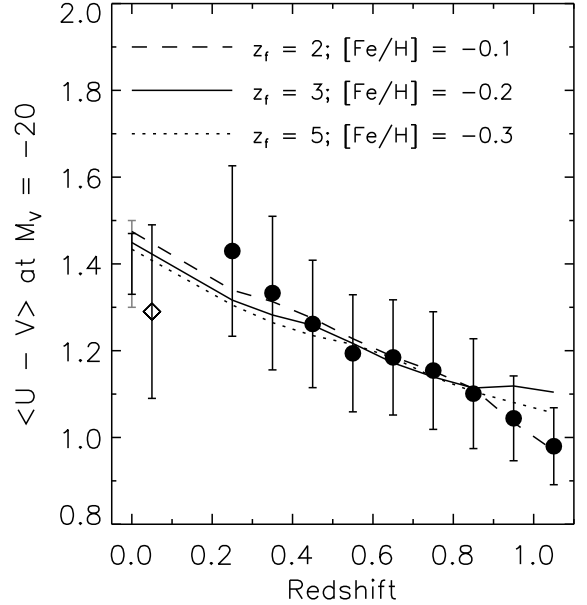


FIG. 2.— Color evolution of the ‘red sequence’, represented by the intercept of the CMR fits at $M_V - 5 \log_{10} h = -20$ (solid circles) as a function of redshift. The error bars show the biweight scatter in each redshift bin. Because of possible small systematic errors in photometric redshift we choose to show this overestimated error to illustrate the worst possible case. The lines show the expected color evolution of single-age stellar populations with different formation redshifts and metallicities, as given in the Figure legend. The diamond with error bars (offset from zero redshift for clarity) shows the $z = 0$ $U - V$ CMR zero point synthesized from SDSS *ugr* data analyzed in the same way as these data (see the Appendix for details). The naked error bars show the $U - V$ CMR zero point for the Abell 754 galaxy cluster (McIntosh, Rix, & Caldwell 2003), which is also consistent with the Nearby Field Galaxy Survey (Jansen et al. 2000) early-type galaxy CMR. The black naked error bar shows the Abell 754 scatter around the CMR, and the expected systematic uncertainty is shown by a grey error bar.

the model colors are insensitive to the choice of stellar initial mass function (IMF), for which we adopt the Salpeter (1955) parameterization in what follows. We show also the color of the CMR intercept from two local samples. The color intercept of morphologically-classified early-type galaxies in the Abell 754 galaxy cluster is shown by the naked error bars (McIntosh, Rix, & Caldwell 2003). This color intercept is consistent with early-type galaxies from a wide range of environments from the Nearby Field Galaxy Survey (Jansen et al. 2000; McIntosh, Rix, & Caldwell 2003). The $U - V$ CMR intercept synthesized from SDSS Early Data Release (EDR; Stoughton et al. 2002) *u*, *g*, and *r*-band data is shown by the diamond with error bars, which is offset from zero redshift for clarity. The SDSS EDR sample is discussed in the Appendix.

The color evolution of the COMBO-17 CMR intercept (the $\langle U - V \rangle$ at $M_V - 5 \log_{10} h = -20$) is consistent with the expectations of passive evolution of ancient stellar populations. However, the COMBO-17 points do seem slightly high compared to the local data, especially at $z \lesssim 0.5$. Absolute calibration of surveys is challenging at even the $\sim 10\%$ level, especially as all of the data shown in Fig. 2 have been transformed to $U - V$ from other passbands, except for the Abell 754 data from McIntosh, Rix, & Caldwell (2003). Furthermore, the number of red-sequence galaxies is low at $z \leq 0.4$, increasing the uncertainties considerably (see Fig. 1). Finally, and perhaps most importantly, color gradients will affect this analysis at some level. The COMBO-17 colors are measured using adaptive-aperture

photometry, and are essentially small-aperture central colors. For the most distant galaxies this will approximate total color. For the nearest COMBO-17 galaxies at $z \lesssim 0.4$, we may sample just their inner, redder parts. Taking typical color gradients from Peletier et al. (1990) as a guide, this could easily lead to a ~ 0.1 mag reddening of the CMR intercept at low redshift compared to the passive evolution expectation from high redshift. The local surveys we show use colors derived for between 50% and 100% of the galaxy light, and this would also lead to an offset between the lowest- z COMBO-17 and local color intercepts at around the ~ 0.1 mag level. Both of these effects are arguably seen in the data. Nevertheless, taken as an ensemble, the CMR intercepts do appear to redden with time in a way that is consistent with the expectations of passive evolution. Yet, even extending large samples to $z \sim 1$, it is not possible to constrain meaningfully the formation redshift of the *stars* in early-type galaxies using this type of information, owing both to the age-metallicity degeneracy, and to systematic model uncertainties of at least $\sim 10\%$ in the colors of old stellar populations (Charlot, Worthey, & Bressan 1996). This is illustrated in Fig. 2, where we choose stellar populations of different ages, with their metallicity at $M_V - 5 \log_{10} h = -20$ adjusted to keep the average $U - V$ color evolution roughly constant.

It is worth briefly discussing some of the structure and scatter in the CMR of early-type galaxies. In the local Universe, the scatter in the CMR is observed to be small ($\lesssim 0.04$ mag; Bower, Lucey, & Ellis 1992; Terlevich, Caldwell, & Bower 2001). This has been interpreted as evidence for a small age spread in local Universe early-type galaxies, although Trager et al. (2000) argue that age and metallicity effects can conspire to produce a small CMR scatter even with large, anti-correlated scatter in age and metallicity. We find rather larger scatter (Fig. 1), mostly because our photometric redshift errors of $\Delta z \sim 0.03$ translate into errors in the derived rest-frame colors of $\Delta(U - V) \sim 0.1$ mag. In addition, the red sequence at $z \lesssim 0.4$ is poorly defined, leading to larger uncertainties. There is also substructure in some (low-redshift) red-sequences; this is especially apparent in the bin at $0.3 < z \leq 0.4$, where some red early-type galaxies form a second CMR. These galaxies are from all three fields, indicating that this is not simply a cluster of galaxies with an offset CMR. Rather, this reflects small, non-random photometric redshift errors, where galaxies from lower redshifts are mistakenly assigned a redshift in this interval. These errors do not significantly affect our results, as we show the full $\pm 1\sigma$ scatter in Fig. 2 (showing the full possible effect of systematic bias), and because the color-selection criteria of $\Delta(U - V) = 0.25$ mag that we choose later in §5 is larger than the scatter at all redshifts (0.09–0.2 mag).

5. THE LUMINOSITY DENSITY OF RED-SEQUENCE GALAXIES

Because the stellar populations of red-sequence/early-type galaxies may have formed much earlier than they were assembled into recognizable early-types (Baugh, Cole, & Frenk 1996; van Dokkum & Franx 2001), the evolution of the CMR, or of the stellar mass-to-light ratios of red galaxies, is not a sensitive diagnostic of when these galaxies attained their present configuration. A much more sensitive diagnostic is the density or luminosity functions of red-sequence galaxies at redshifts less than unity.

In §§3 and 4, we have seen that it is possible to define the early-type galaxy population in an empirical, model-independent fashion by exploiting the bimodality of the galaxy color distribution out to $z \sim 1$ (Fig. 1). We therefore choose to study

galaxies around the red galaxy CMR, defining these as the red-sequence galaxy population at any given redshift. More quantitatively, we define red-sequence galaxies as being redder than $\langle U - V \rangle = 1.18 - 0.38z - 0.08(M_V - 5 \log_{10} h + 20)$ (the dashed line in Fig. 1). This line is roughly 0.25 mag bluewards of a rough by-eye fit to the evolution of the mean color of a $M_V - 5 \log_{10} h = -20$ galaxy from Fig. 2. We choose this definition merely to have a criterion that is a continuous function of redshift. Using a discontinuous color-cut which is 0.25 mag bluewards of the empirical CMR zero-point defined within each $\Delta z = 0.1$ bin yields results that agree within the errors. Our color-cut philosophy is similar to that of Butcher & Oemler (1984), except that we choose to keep the red galaxies rather than the blue ones. The advantages of this definition of early-type galaxies are many. Firstly, it is straightforward to match this selection criterion in theoretical models. For example, even if the model CMR is curved, one can simply go ~ 0.25 mag redwards of the curved locus in $U - V$ space and choose galaxies redder than that curved locus (although as long as the ‘gap’ between the red and blue peaks is sparsely populated, like in the observational data, the exact choice of color cut makes little difference as long as the cut lies in the ‘gap’). Secondly, it automatically accounts for evolution in a model-free way by fitting the CMR ridge-line. Thirdly, this definition has a well-defined physical meaning (galaxies that have colors consistent with old stellar populations at a given redshift). A final advantage is this definition’s insensitivity to differences in photometric zero points. For example, the local SDSS comparison sample and COMBO-17 sample may have offset $U - V$ color scales (Fig. 2); yet, the B -band luminosity density of galaxies on the CMR is insensitive to this small color offset, meaning that the luminosity density of the local SDSS sample can be meaningfully compared with the rest-frame B -band luminosity density of the COMBO-17 dataset. We note that this definition contrasts with W03, who adopted spectral type definitions based on present-day spectral energy distribution types. With this new approach, we are taking into account in a natural and empirical way the effects of evolution in red sequence galaxy color.

Defining galaxy types in this way, we now explore the evolution of the luminosity function of COMBO-17 red-sequence galaxies in Fig. 3. We estimate the galaxy luminosity function in different redshift bins following W03 using the V/V_{\max} formalism (e.g., Felten 1977), using our detailed estimates of galaxy completeness as a function of surface brightness, magnitude, redshift and spectral type (see, e.g., Figs. 6 & 7 of W03). Schechter (1976) functions were fit to the red-sequence galaxy sample using the method of Sandage, Tammann, & Yahil (1979, STY hereafter). We choose to fit the entire red-sequence galaxy sample at all redshifts with one common value of the faint-end slope α ; in practice, α is determined mainly by the low-redshift galaxy samples and is -0.9 ± 0.1 in this case. The magnitude at the ‘knee’ of the luminosity function (M^*) is redshift, but not field-to-field, dependent, and the density normalization ϕ^* is fit separately to each field at each redshift. The Schechter luminosity function to the local comparison sample is shown by a dotted line (see the Appendix for more details).

W03 found strong evolution of ‘early-type galaxies’, defined via redshift-independent spectral energy distribution criteria (which did not take into account galaxy evolution). In contrast, one can see from Fig. 3 that the luminosity function evolution of early-type galaxies defined in this way is remarkably mild. The characteristic magnitude M^* brightens slightly

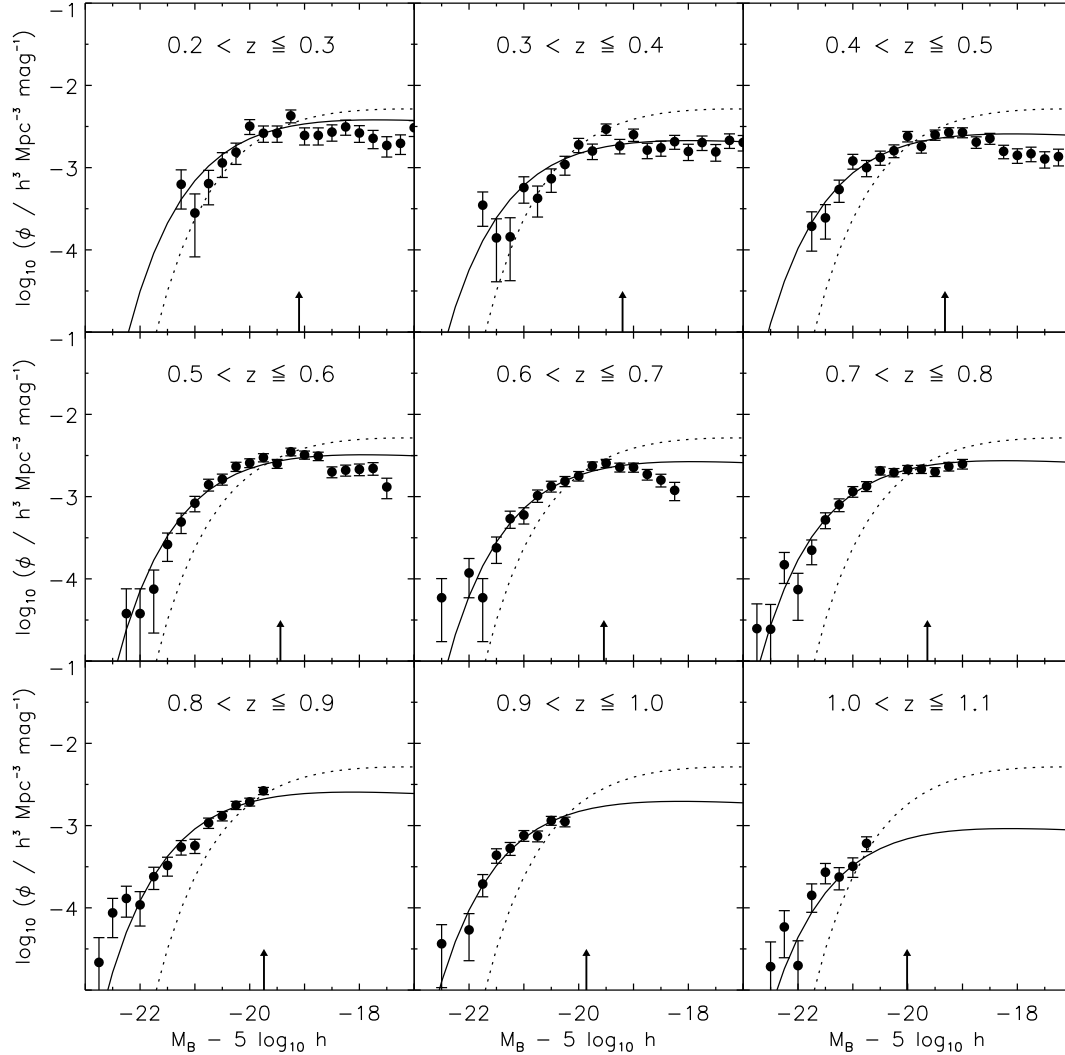


FIG. 3.— Redshift evolution in the luminosity function of res-sequence galaxies. Black solid lines with data points show the Schechter Function fits and V/V_{\max} luminosity functions of COMBO-17 red-sequence galaxies in each redshift interval. The dotted line shows the Schechter fit to the low-redshift SDSS comparison sample (see the Appendix for more details). A single faint-end slope $\alpha = -0.9$ is derived by a single STY fit to the COMBO-17 data at all redshifts. Note how little this luminosity function changes for $M_B \gtrsim -21$. The arrow shows the magnitude cutoff used for the analysis of the luminous red-sequence galaxy population in §6.4, assuming $z_f = 3$.

with increasing redshift; yet, the abundance of galaxies with luminosities below M^* remains virtually unchanged.

We quantify this mild evolution in Fig. 4, where we show the redshift evolution of the luminosity density of the red-sequence galaxy population. The luminosity density is estimated by integrating the best-fit Schechter Function to infinity using $j = \phi^* L^* \Gamma(2 + \alpha)$. We show the average luminosity density (open circles) with an error bar showing the full range of luminosity density derived from the three different fields. For most bins this will give a conservative estimate of the systematic error from large-scale structure. We show also a lower limit to the luminosity density, derived only from the observed luminosity density without extrapolating to zero luminosity (upwards-pointing triangles). The redshift zero point (solid circle) is from a sample of SDSS EDR galaxies which have been selected using the same method on synthesized $U-V$ colors (Bell et al. 2003, see the Appendix). We show also the 2dFGRS data point of spectral-type selected early-type galax-

ies (Madgwick et al. 2002) as an filled grey circle. The error bar extends further to lower luminosity density because Madgwick et al. (2002) do not account for evolution (which may bias both the magnitude and density normalization upwards; Blanton et al. 2001). The smooth grey lines show the expectation of passive evolution models, normalized to go through the redshift zero SDSS data point. The model evolution is insensitive to stellar IMF at the 0.1 mag level.

This figure shows a few key results. Firstly, there is significant field-to-field variation in red sequence luminosity density, even between the three ~ 0.25 square degree COMBO-17 fields. Thus, large scale structure is the limiting uncertainty for our and similar studies of the evolution of the luminosity function of red-sequence or early-type galaxies between $0 < z \lesssim 1$. Therefore, it will be necessary to cover substantially larger areas to similar depths to significantly improve on these results. Secondly, and most importantly, the rest-frame B -band luminosity density in red-sequence galaxies remains more or less

TABLE 2
RED GALAXY LUMINOSITY FUNCTION SCHECHTER FITS AND CMR INTERCEPT

$\langle z \rangle$	$M^* - 5 \log h$ (Vega mag)	$\phi^* \times 10^{-4}$ (h/Mpc) $^{-3}$	$j \times 10^7 L_\odot$ (h/Mpc^3)	f_{obs}	c_{ϕ^*, L^*}	$(U-V)_{M_V=-20}$
0.25	-20.19 ± 0.27	53.02 ± 26.48	8.53 ± 4.26	0.99	-0.384	1.43 ± 0.20
0.35	-20.47 ± 0.28	29.65 ± 10.94	6.20 ± 2.29	0.98	-0.349	1.33 ± 0.18
0.45	-20.59 ± 0.32	35.78 ± 11.78	8.32 ± 2.74	0.97	-0.336	1.26 ± 0.15
0.55	-20.42 ± 0.27	44.90 ± 6.68	8.92 ± 1.33	0.93	-0.392	1.19 ± 0.13
0.65	-20.43 ± 0.17	37.05 ± 16.99	7.47 ± 3.42	0.87	-0.530	1.18 ± 0.13
0.75	-20.73 ± 0.16	38.05 ± 8.02	10.11 ± 2.13	0.81	-0.653	1.15 ± 0.13
0.85	-20.64 ± 0.20	35.52 ± 21.38	8.69 ± 5.23	0.64	-1.022	1.10 ± 0.13
0.95	-20.64 ± 0.18	27.40 ± 12.11	6.67 ± 2.95	0.49	-1.390	1.04 ± 0.10
1.05	-20.64 ± 0.23	12.80 ± 5.44	3.10 ± 1.32	0.33	-1.964	0.98 ± 0.09

Note. — STY fits in 9 redshift intervals; the faint end slope $\alpha = -0.9 \pm 0.1$ was fit to the entire sample. Listed are M^* , ϕ^* with its field-to-field variation, the luminosity density j , the fraction of the luminosity density that is constrained by the measurements, and the covariance between ϕ^* and M^* . Also given is the intercept of the CMR at $(U-V)$ color at $M_V = -20$ and the robust biweight RMS scatter.

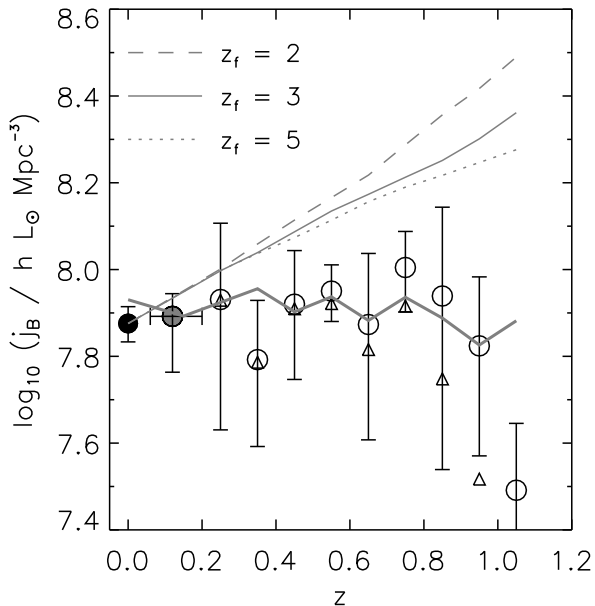


FIG. 4.— The evolution of the rest-frame B -band luminosity density of the red-sequence galaxy population from COMBO-17. The rest-frame B -band luminosity density per comoving Mpc^3 is shown by open circles, with error bars denoting the large field-to-field variations because of large-scale structure. The upwards-pointing triangles denote a lower limit to the luminosity density, if only the observed luminosity density is accounted for (i.e., no extrapolation to zero luminosity). The solid point shows the SDSS B -band luminosity density of red-sequence galaxies (transformed from ugr data; the Appendix) and the filled grey point is the early-types in the 2dFGRS selected by the spectral-type parameter η . We show the expectations of a passive evolution model as smooth grey lines (with formation redshift shown in the Figure legend). We show also the blind prediction of the Cole et al. (2000) semi-analytic galaxy formation model as a thick solid grey curve.

constant over the interval $0 < z \lesssim 1$. The observed luminosity density falls short of the passive evolution prediction by a factor of two or three by $z \sim 1$, although the significant field-to-field scatter precludes a more accurate assessment. We note that we

place little weight on the apparent sudden decline in the j_B in the final $1 < z \leq 1.1$ bin, owing to uncertainties in the factor-of-three extrapolation to total luminosity density, incompleteness correction uncertainties, and photometric redshift uncertainties for these faint $m_R \gtrsim 23$ galaxies.

Of pivotal importance in establishing this result is the local estimate of red sequence luminosity density. This was the primary motivation for carefully constructing a SDSS comparison sample. As discussed in Bell et al. (2003), this estimate is accurate to 10% in a systematic and random sense, owing largely to the excellent completeness properties of SDSS (used for galaxy selection) and the Two Micron All Sky Survey (which is used to normalize the luminosity function to the all-sky number density of $10 < K < 13.5$ galaxies). Furthermore, the $U-V$ colors were synthesized to allow identical selection criteria to be applied to the low-redshift and COMBO-17 samples, strongly limiting that source of systematic uncertainty. Furthermore, the 2dFGRS estimate of Madgwick et al. (2002) agrees with our SDSS estimate, lending further credibility to the low-redshift comparison data. Therefore, we believe that it is safe to conclude that the rest-frame B -band luminosity density of color-selected early-type galaxies does not significantly evolve in the interval $0 < z \lesssim 1$. Furthermore, because a passively-evolving population would have to fade by a factor of two or three from redshift one to the present day in rest-frame B -band, this non-evolving j_B corresponds to an increase in stellar mass in red galaxies of a factor of two to three from redshift unity to the present day.

6. DISCUSSION

6.1. Comparison with previous work

The data presented here are based on a larger galaxy sample than all previous work in this field combined. Furthermore, we adopt an empirically-motivated definition of ‘early-type galaxy’ which accounts for evolution of the stars in these galaxies in a natural and model-independent fashion. Nevertheless, on the whole there is pleasing agreement between our

conclusions and the results of many of the previous studies of this topic. The essentially passive evolution of the *stars* in early-type galaxies (not the galaxy population as a whole), as estimated from the color intercept of the CMR, is in excellent agreement with the colors (e.g., Kodama & Arimoto 1997; Kodama, Bower, & Bell 1999; van Dokkum et al. 2001), line strengths (e.g., Kuntschner 2000; Kelson et al. 2001; Ziegler et al. 2001), and stellar M/Ls (e.g., van Dokkum & Franx 2001; Treu et al. 2002) of individual early-type galaxies between $0 \lesssim z \lesssim 1$, as extensively discussed in the introduction.

There is also good agreement between our detection of a factor of two evolution in stellar mass on the red sequence and other works in the literature. Morphologically-selected surveys (Im et al. 1996; Schade et al. 1999; Menanteau et al. 1999; Im et al. 2002) found little evidence for density evolution given the small sample sizes ($\lesssim 150$ galaxies) and cosmic variance, and could not rule out passive or mild evolution of the type that we see. Interestingly, they found evidence for blue cores in some morphologically early-type galaxies, perhaps lending credibility to a ‘frosting’ model of early-type evolution at $0 \lesssim z \lesssim 1$, as discussed by Trager et al. (2000, although see §6.4).

Most color-selected surveys also agree with our conclusions. Lilly et al. (1995) study evolution in the luminosity function of galaxies with colors redder than a present-day Sbc galaxy; this color lies at the red end of the blue distribution at all redshifts because the blue sequence does not change in color. They find very little evolution, with large uncertainties from small number statistics and large-scale structure, which is consistent with both our result and passive evolution. Kauffmann et al. (1996) re-analyse this result, finding a factor of three evolution in galaxies with the colors of early-types, although Totani & Yoshii (1998) point out that spectroscopic incompleteness affects this result. Lin et al. (1999) agree with this picture using a similar technique with a larger sample of galaxies over a more restricted redshift range. Pozzetti et al. (2003) used the K20 survey to estimate the evolution of red galaxies out to $z \sim 1$; using a total galaxy sample of only 546 galaxies from 52 square arcmins, they find mild evolution in the number of luminous red galaxies, but with error bars of a more than a factor of two (not accounting for the dominant uncertainties from large scale structure). Chen et al. (2003) have used the Las Campanas Infrared Survey to estimate the luminosity density evolution of red galaxies in the rest frame *R*-band, finding at most a factor of a few evolution in red galaxy density, although they were not able to rule out passive evolution with their sample. We are consistent with these results, but have been able to place much stronger constraints based on our factor of at least three improvement in sample size and factor of two larger sky coverage, compared to the largest of the previous works. Importantly, these previous works often neglected the uncertainties stemming from large-scale structure; we alone are able to quantify this dominant source of uncertainty because of our large sky coverage over three disjoint fields.

Finally, we should compare with our own earlier work, W03, where we explored the same COMBO-17 dataset, but used a conceptually different, non-evolving definition of ‘early-type galaxies’ (their type 1). Their non-evolving spectral typing corresponds to constant rest-frame color cuts at all redshifts; their type 1 corresponds to $U - V \gtrsim 1.35$, and their type 2 corresponds to $1.35 \gtrsim U - V \gtrsim 0.95$. Thus, type 1 galaxies have the colors of present-day luminous elliptical and lenticular galaxies, but are significantly redder than the reddest galaxies at

higher redshift. Consequently, W03 found rapid evolution of type 1s, in the sense that galaxies with the colors of present-day early-types are extremely rare in the distant Universe (because of passive evolution) Because of these definition differences, the statement by W03 that galaxies redder than a fixed threshold have a rapidly evolving luminosity density is consistent with our statement of a roughly non-evolving rest-frame *B*-band luminosity density in red-sequence galaxies.

In summary, all of our results are consistent with those presented to date in the literature, but with much greater precision and understanding of the uncertainties owing to our factor of $\gtrsim 3$ larger sample and sky coverage.

6.2. The Nature of Red Galaxies

We now turn to the nature of galaxies in this red population: are these galaxies red because they contain almost exclusively old stars, or is there a significant contribution from more dusty, star-forming galaxies?

At low redshift, the red population is overwhelmingly composed of morphologically early-type galaxies (e.g., Sandage & Visvanathan 1978; Bower, Lucey, & Ellis 1992; Schweizer & Seitzer 1992; Terlevich, Caldwell, & Bower 2001; Hogg et al. 2002). For the SDSS survey, Strateva et al. (2001) find that $\sim 80\%$ of the red galaxies are earlier than Sa in morphological type.

At intermediate redshift, most studies have targeted dense environments: in intermediate redshift clusters most red or non-star-forming galaxies are spheroid dominated (e.g., Couch et al. 1998; van Dokkum et al. 2000; van Dokkum & Franx 2001). Furthermore, most of the luminosity density of morphologically-classified early-type galaxies in the Hubble Deep Field North at $z \sim 0.9$ is in red-sequence galaxies (Kodama, Bower, & Bell 1999).

At higher redshift, a number of studies have explored the nature of ‘extremely red objects’ (EROs), which have very red colors consistent with passively-evolving ancient stellar populations with $1 \lesssim z \lesssim 2$. Cimatti et al. (2002) use deep spectroscopy to split EROs roughly 50:50 between passively-evolving red-sequence galaxies and dusty star-forming galaxies in $K \leq 19.2$ sample of 45 EROs. A complementary technique is adopted by Yan & Thompson (2003), who use *Hubble Space Telescope* (HST) imaging, finding that to $K = 19$, $\sim 65\%$ of EROs have disk morphologies (and are primarily dust-reddened edge-on galaxies) while only $\sim 35\%$ have bulge-dominated morphologies. Furthermore, some of each class (including $\sim 1/3$ of bulge-dominated galaxies) have disturbed morphologies, suggesting an interaction, perhaps with an accompanying dusty starburst.

This evidence suggests that most red galaxies to $z \lesssim 1$ are morphologically early-type with dominant old stellar populations. In contrast, a significant fraction of distant $z \gtrsim 1$ red galaxies may have red colors not because of a dominant old stellar population, but rather because of dust (i.e., edge-on disks or dusty starbursts). This implies that our results should be interpreted as upper limits on the abundance of galaxies dominated by ancient stellar populations until the advent of more definitive morphological data and/or spectra for sufficient numbers of galaxies with $0.2 \lesssim z \lesssim 1$. Work is ongoing with the *Galaxy Evolution from Morphology and SEDs* project (GEMS²; Rix et al. 2003, in preparation), which uses the HST Advanced Camera for Surveys to mosaic the entire COMBO-17 CDFS area in

²<http://www.mpia.de/homes/barden/gems/gems.htm>

606W and 850LP passbands. This survey will ultimately allow morphological classification for $\gtrsim 2000$ red-sequence galaxies, powerfully constraining the nature of these galaxies out to $z \sim 1$. Indeed, preliminary work with the 850LP images suggests that the vast majority of the luminosity density in red-sequence galaxies at $z \sim 0.65$ is from bulge-dominated galaxies, which would validate the utility of this empirically-motivated color selection out to at least that redshift (Bell et al. 2003, in preparation).

6.3. The Predicted Luminosity Evolution of Hierarchical Model Galaxies

In §5 we showed that the rest-frame B -band luminosity density of red-sequence galaxies does not significantly evolve since $z \sim 1$. This is at variance with the expectations of a completely passive evolution model (where red-sequence galaxies fully form at $z \gg 1$ and simply age to the present day), which would predict a factor of two or three decrease in the rest-frame B -band luminosity density in red galaxies from redshift one to zero. It is interesting to compare our results with the expectations of hierarchical models of galaxy formation and evolution, to check if these models would predict a roughly non-evolving B -band luminosity density since $z \sim 1$ in red galaxies.

There are two main predictions of hierarchical models of galaxy formation and evolution. Firstly, early-type galaxies in the field should have stellar population of a somewhat younger mean stellar age, and they should be assembled later than their clustered counterparts, because the mergers which give rise to the early-types happened at earlier times in clusters than in the field (where they continue even to the present day; e.g., Baugh, Cole, & Frenk 1996). We have chosen not to explore this issue at present, as constructing local density estimators with a redshift precision of $\Delta z \sim 0.03$ is non-trivial; we will explore environmental dependence of galaxy colors in a future work. Other studies may have detected an offset, in the sense that field early-types may be younger than cluster early-types, using line strength (Guzman et al. 1992; Bernardi et al. 1998) or fundamental plane constraints (Treu et al. 2002). Nevertheless, progenitor bias is a significant observational worry in studies of this kind, and more work is required to firm up these interesting results. A particularly exciting avenue of research is study of mass-selected galaxies from gravitational lensing studies. In these studies, the sample is selected to have high stellar+dark masses, without regard for their photometric properties (or indeed, for their environments). First results from these surveys have been controversial but promising. Kochanek et al. (2000) and Rusin et al. (2003) find no evidence for younger stellar populations in (the same) mass-selected sample, compared to galaxy clusters. van de Ven, van Dokkum, & Franx (2003) re-analyze these data using a more model-dependent but sensitive approach, accounting for progenitor bias, finding younger luminosity-weighted ages than clustered massive galaxies, in agreement with hierarchical model expectations.

The second main prediction of hierarchical models of galaxy formation is a gradual increase in the stellar mass of the early-type/red-sequence galaxy population up until the present day, because of constant build-up in stellar mass from galaxy mergers (Baugh, Cole, & Frenk 1996; Kauffmann et al. 1996). In Fig. 4, we show a blind prediction of the Cole et al. (2000) fiducial model using the same color-magnitude relation methodology adopted in this paper. The models are constrained to match the local luminosity function plus the morphological mix of

$L \gtrsim L^*$ galaxies in the local Universe, therefore the match between the models and the observations at redshift zero is largely by design. Observations of luminosity functions at non-zero redshifts were not used at any stage to constrain model parameters, therefore the excellent agreement between the model and the data out to $z \sim 1$ is a significant achievement. This match is non-trivial; Somerville & Primack (1999) models do not match the data well (Somerville 2003, priv. comm.), and predict a much stronger evolution of j_B with redshift, such that red-sequence galaxies at $z \sim 1$ are very rare indeed, even with our evolving type definition. The origin of this discrepancy is the well-known inability of models of this type to match both the dynamics and luminosity functions of galaxies simultaneously. The Cole et al. (2000) model tunes to match the luminosity function of galaxies well at the present day, and is therefore the suitable model with which to compare luminosity density evolution. The Somerville & Primack (1999) model (and, for reference, the Kauffmann et al. 1999, model) tunes to reproduce galaxy dynamics at the expense of the galaxy luminosity function, and is less suitable for comparisons of this type (but is more suitable for estimating the cosmic evolution of galaxy dynamics). A more thorough discussion of the stellar mass, dynamical and morphological evolution of the red-sequence galaxy population is clearly warranted, but is beyond the scope of this paper. Nevertheless, the current zero-order comparison is rather encouraging; models that are tuned to reproduce the present-day distribution of galaxy luminosities predict no evolution in the luminosity density of red-sequence galaxies, in agreement with our observations.

6.4. The Origin of Luminous Red-Sequence Galaxies

What might these data tell us about the origin of luminous red-sequence galaxies? As a useful tool for this discussion, we construct a sequence of PÉGASE model galaxies with truncated SFHs (the solid lines with crosses in Fig. 1). We construct a ‘bright’ ($M_V - 5 \log_{10} h \sim -21$) and ‘faint’ ($M_V - 5 \log_{10} h \sim -19$) set of model galaxies. These models are not designed to be particularly realistic, rather they are designed to show what a galaxy with a given stellar mass at the redshift of interest would look like if it had its SFH stopped (the second-bluest to the reddest crosses on each track), compared to one which had star formation (SF) continuing to the present-day (the bluest cross on each model galaxy track). We discuss the ‘bright’ set of model galaxies first, discussing the ‘faint’ set afterwards. The ‘bright’ set of model galaxies is based on a galaxy with a SFH of the form $\psi \propto e^{-t/\tau}$, where ψ is the star formation rate (SFR), t is the time elapsed since galaxy formation, and τ is the e -folding time of the SFH, set in this case to be 4 Gyr. The formation redshift is assumed to be $z_f = 2$, and the metallicity is assumed to be constant at solar, for simplicity. The evolution of this model with cosmic time is shown by the bluest cross on the ‘bright’ track in each panel of Fig. 1.

The solid line at $M_V - 5 \log_{10} h \sim -21$ in each panel of Fig. 1 connects this $\tau = 4$ Gyr model with models which have the identical SFH (crosses), except that they have had their SF stopped arbitrarily after an elapsed time of 90%, 80%, 50% and 10% of the age of the galaxy at the redshift interval of interest (these models correspond to the second bluest cross to the reddest cross, respectively; the bluest cross is the untruncated model as discussed above). When the SF is stopped, a burst of SF occurs which increases the stellar mass of the truncated model to the same stellar mass as the untruncated galaxy. The ‘faint’ set

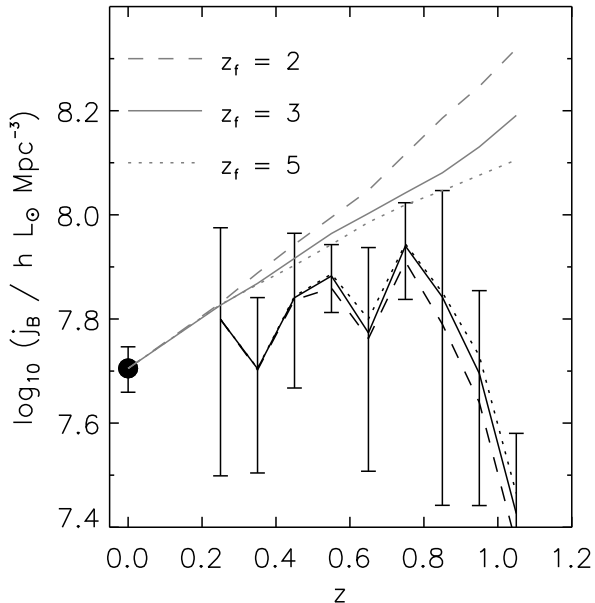


FIG. 5.— The luminosity density evolution of luminous red-sequence galaxies. The luminosity density of those red-sequence galaxies destined to evolve passively into galaxies brighter than $M_B - 5 \log_{10} h \leq -19.1$ at $\langle z \rangle = 0.25$ is shown in Fig. 5 by dashed, solid and dotted black lines for $z_f = 2, 3, 5$ respectively. The smooth grey curves show the expected evolution of a galaxy population that completely formed at high redshift and simply aged to the present day. The error bars show the full range of uncertainty, as estimated from field-to-field variation in the luminosity density.

of models is analogous, except with 1/3 solar metallicity and a constant SFR ($\tau = \infty$), in order to have the somewhat bluer colors characteristic of fainter galaxies.

A cursory inspection of these tracks in Fig. 1 show clearly that while faint red-sequence galaxies may plausibly be faded remnants of blue, later-type galaxies which exist at the same epoch, there are very few blue galaxies bright enough to fade into the most luminous red-sequence galaxies *at all redshifts out to* $z \sim 1$. Thus, luminous red-sequence galaxies cannot have originated from simple fading of single blue star-forming galaxies since redshift one. This implies that most luminous red-sequence galaxies were either completely formed earlier than $z \sim 1$, or that these luminous red-sequence galaxies formed through mergers of galaxies.

We explore these two possibilities by considering the luminosity density in luminous red-sequence galaxies at $z \lesssim 1$. Let us adopt as a null hypothesis that luminous red-peak galaxies form completely at high redshift and simply age to the present day (the first option). Then, if we choose to evaluate the luminosity density in red-sequence galaxies above a passively-fading luminosity cut (i.e., a constant stellar mass cut), we should observe a luminosity density which fades passively (like the grey passive evolution tracks in Figs. 4 and 5). If the total luminosity density in this sub-population does not follow a simple fading track, then a merger origin for at least some of the luminous red galaxies at $z \lesssim 1$ appears necessary (the second option) to boost this population of luminous red galaxies. In order to place the most interesting constraints, we choose a luminosity cut corresponding roughly to the ‘bright’ $M_V - 5 \log_{10} h \sim -21$ track in Fig. 1 above which there are few blue galaxies which can fade onto the red sequence.

The luminosity density of red-peak galaxies destined to passively evolve into galaxies brighter than $M_B - 5 \log_{10} h \leq -19.1$

at $\langle z \rangle = 0.25$ (as calculated using the rate of fading of PÉGASE model stellar populations in conjunction with an assumed formation redshift) is shown in Fig. 5 by dashed, solid and dotted black lines for different formation redshifts $z_f = 2, 3, 5$. This luminosity cut is equivalent to $M_V - 5 \log_{10} h \leq -20$, accounting for the average rest-frame color of red-peak galaxies at that redshift of $B - V = 0.9$. We show example cuts as a function of redshift in Fig. 3 as arrows, assuming $z_f = 3$. For reference, these example cuts are $M_B - 5 \log_{10} h \leq -19.1, -19.2, -19.32, -19.44, -19.54, -19.64, -19.74, -19.86, -20.01$ for $\langle z \rangle = 0.25, 0.35, 0.45, 0.55, 0.65, 0.75, 0.85, 0.95, 1.05$, again for $z_f = 3$. We overplot large scale structure errors, as before. We show also the luminosity density in galaxies brighter than $M_B - 5 \log_{10} h \leq -18.8$ at $z = 0$ for SDSS EDR red-peak galaxies as a solid point; this cutoff corresponds to $M_B - 5 \log_{10} h \leq -19.1$ at $\langle z \rangle = 0.25$, passively faded to the present day. The passive fading expectation is shown in the grey lines. The luminosity densities are sums of the V/V_{\max} points, except for a tiny contribution to the two highest redshift bins, where we must extrapolate slightly using the Schechter function fit.

It is clear that the observed luminosity density in *luminous* red peak galaxies evolves relatively little over the interval $0 \lesssim z \lesssim 1.1$. There is perhaps a modest increase out to $z \sim 0.7$, then a significant drop at higher redshift. This weak evolution does not agree with the expectations of passive evolution models (where the galaxy population forms completely at high redshift and simply ages to the present day). Thus, the population of luminous red-peak galaxies (those destined to become red-peak galaxies with $M_B - 5 \log_{10} h \leq -19.1$ by $\langle z \rangle = 0.25$) grows in stellar mass by roughly a factor of two in the interval $0 < z \leq 1.1$. There is a hint that much of this stellar mass build-up happens at $z \gtrsim 0.7$, with a modest gradual increase at later times. Clearly, however, a larger survey with lower uncertainties from large scale structure is required to further constrain the epoch of rapid stellar mass assembly in the luminous red galaxy population.

The significance of the evolution in the *luminous* red galaxy population is that we have chosen a luminosity cutoff which corresponds to the ‘bright’ truncation model of Fig. 1. At all redshifts, it is clear that there are very few single blue galaxies bright enough to fade into a red galaxy with luminosities brighter than this model. Yet, this luminous red galaxy population builds up in stellar mass by a factor of two in this redshift range. Red massive progenitors would have been included in the luminosity density estimates, and blue massive progenitors are observed to be very rare indeed (Fig. 1). Thus, merging between less luminous galaxies is required to build up these luminous red galaxies. Furthermore, owing to the rarity of luminous blue galaxies, these mergers must have at most a very brief luminous blue phase. This is possible if most mergers of massive galaxies are either very dusty (obscuring and reddening the stellar populations until the stellar populations age and redden sufficiently to join the red sequence) or are very gas poor to begin with (e.g., the elliptical-elliptical mergers observed by van Dokkum et al. 2001, and explored theoretically by Khochfar & Burkert 2003). Exploring these two options in detail is far beyond the scope of this work, except to note that both have clear observational signatures. The highly-obscured gaseous mergers should be among the brightest far-infrared sources at any given redshift, and will therefore be well-constrained by current and planned observations in the far-infrared and sub-mm regime. On the other hand, the elliptical-elliptical mergers, if they build

up the galaxy mass by more than a factor of two or so, will flatten the CMR at the highest luminosities (Bower, Kodama, & Terlevich 1998). Disentangling the contributions from both processes will be a fascinating prospect for the coming years.

The distribution of galaxy colors also strongly constrains the ‘frosting’ model of Trager et al. (2000). In this scenario, many early-types have residual low-level SF at $z \lesssim 1$. One could postulate that the factor of two evolution in stellar mass in red-sequence galaxies is due to residual SF in the other half of the galaxies, making them too blue to satisfy our redshift-dependent color cut. This residual SF slows to the present day, giving an apparent evolution of a factor of two in stellar mass while avoiding the need for wholesale galaxy assembly through galaxy mergers. However, this mechanism could not work for at least high-luminosity red galaxies. A ‘frosting’ of SF on top of a massive red-sequence galaxy at $z \sim 1$ would produce an even brighter blue galaxy, in clear contradiction with the observations. Indeed, as estimated using the PÉGASE stellar population model, a color difference of $\Delta(U-V) \sim 0.25$ (the color cut adopted in our definition of red-sequence galaxies) corresponds to an ongoing SF rate of only a few percent of the average SF rate at earlier times (i.e., the birthrate $b = \text{SFR}/\langle \text{SFR} \rangle < 0.05$, where SFR is the SF rate). Thus, the observations strongly limit the amount of residual SF in massive red-sequence galaxies all the way from $z \sim 1$ to the present day to less than a few percent enhancement in stellar mass over the whole redshift range $0 < z \leq 1.1$. Our observations say little about less luminous early-types; medium-to-high resolution, high S/N spectroscopy, or perhaps constraints from the rest-frame near-infrared using the *Space InfraRed Telescope Facility* will allow us to more meaningfully constrain the SFHs of less luminous red-sequence galaxies.

6.5. A Synthesis

It is interesting to bring together some of the different threads in this paper into an overall qualitative, perhaps in parts naive, picture of galaxy evolution.

Firstly, the color distribution is bimodal. As discussed above at the end of §6.4, birthrates (the relative present-day SFR compared to the average past SFR) for red-sequence galaxies are low $\lesssim 5\%$. Interesting lower limits on the birthrates of blue-peak galaxies can be derived by assuming that these galaxies are dust-free. Again using the PÉGASE stellar population models, the red end of the blue peak (with $U-V \sim 0.7$) corresponds to $b \sim 0.1$, whereas the bluest galaxies correspond to $b \sim 1$. Thus, galaxies on the blue peak *need not be forming stars vigorously at the present day*. Indeed, modest rates of only 10% of the past average SFR are required to keep a galaxy on the blue peak (more, if the effects of dust are important). Thus, bimodality in the color distribution of galaxies simply betrays the face that young stars are very bright, and that if even a small number of young stars are present they dominate the optical colors of that galaxy. The red peak, in contrast, tells us that there is a ‘glut’ of non-star forming galaxies, with present day SFRs of at most a few percent of their past average SFRs.

Secondly, the *B*-band luminosity density of galaxies in the red sequence does not significantly evolve in the interval $0 < z \leq 1.1$. This implies a build-up of stellar mass on the red peak (this ‘glut’ of non-star formers) by a factor of two since $z \sim 1$. This stellar mass must come from the blue peak galaxies, as we are not permitted to form the stars *in situ* because of the red colors of the red-sequence population.

Is the relative number of galaxies in the red and blue peaks, and in the gap, consistent with this picture? We explore this by constructing a very simplistic model, in which some small fraction of star-forming galaxies in the blue peak are ‘turned off’ (by some unspecified mechanism) and subsequently redden and fade. Fading across the ‘gap’ takes around $\sim 40\%$ of the Hubble time (as seen by the crosses on the fading tracks in Fig. 1). In order to reproduce the roughly factor of two to three difference in the number of galaxies in the gap compared to the blue peak, it is necessary to turn off roughly 5–10% of the blue galaxies per Gyr, letting them fade across the gap. This rate of transformation also gives a factor of roughly two increase in the stellar mass density on the red sequence. Thus, a very simplistic picture where some fraction of the blue population of galaxies have their SF stopped every Gyr (by some unspecified mechanism), subsequently fading into red galaxies, holds water.

Of course, we know that there must be other physical processes at work. A truncation-only model predicts that the characteristic luminosity of red galaxies is fainter than the blue population. Yet, the brightest and most massive present-day galaxies in the Universe are almost all red (e.g., Kochanek et al. 2001; Bell et al. 2003). Furthermore, this situation persists out to $z \sim 1$ (Fig. 1). Another prediction is that the morphologies of the red and blue peak populations should be rather similar, which again is completely ruled out by observations (Strateva et al. 2001). Galaxy mergers are a likely process for rectifying these shortcomings. Galaxy mergers will increase the characteristic luminosity of post-merger galaxies through the addition of the pre-existing stellar populations, in conjunction with any SF associated with the merger itself. Furthermore, the violent relaxation associated with galaxy mergers leads to more spheroidal-dominated morphologies (e.g., Eggen, Lynden-Bell, & Sandage 1962; Toomre & Toomre 1972; Barnes & Hernquist 1996). Indeed, mergers and galaxy interactions may even provide a mechanism for the truncation of SF, through the consumption of the gas in an induced starburst (e.g., Barnes & Hernquist 1996; Barton, Geller, & Kenyon 2000). The only constraint which we can place on the role and frequency of these mergers with these data is that the mergers responsible for the most luminous red galaxies cannot have a long blue phase, owing perhaps to dust or a lack of gaseous content in the progenitors.

This qualitative picture agrees well with many of the features of current models of galaxy formation in a hierarchical CDM Universe (e.g., White & Frenk 1991; Kauffmann et al. 1996; Somerville & Primack 1999; Cole et al. 2000). Furthermore, it makes a number of predictions that are testable in the near future. For example, the merger origin of the most luminous red galaxies can be tested by both deep optical HST imaging over wide fields and by far-infrared and sub-mm deep imaging to constrain the frequency of mergers between gas-poor early types and more gaseous later types, respectively. Additionally, one can test the viability of the truncation model, and constrain truncation mechanisms, through a combination of deep HST imaging (for galaxy morphologies as a function of color and magnitude) and deep spectroscopy (to check for signatures of recently-truncated SF, such as enhanced Balmer absorption lines). Furthermore, one can seek to explore these different galaxy populations in different local environments, to seek the signature of more rapid environmentally-induced transformation in denser environments.

7. CONCLUSIONS

The evolution of red-sequence/early-type galaxies directly reflects the importance and number of major galaxy mergers, and therefore strongly constrains hierarchical models of galaxy formation and evolution. We have explored the rest-frame colors and luminosities of $\sim 25000 R \lesssim 24$ galaxies from 0.78 square degrees from the COMBO-17 survey, encompassing a cosmologically-representative total volume of $\sim 10^6 h^{-3} \text{Mpc}^3$. We find that the distribution of galaxy colors is bimodal at all redshifts out to $z \sim 1$.

The blue star-forming peak has colors that do not strongly vary with redshift; however, there are many more luminous blue galaxies at $z \gtrsim 0.5$ than there are at the present day (this is discussed in much more detail by Wolf et al. 2003).

The red non-star-forming peak forms a well-defined color-magnitude relation (CMR) at $0.2 < z \leq 1.1$, with luminous galaxies being redder than their fainter counterparts, as is observed in galaxy clusters with $0 < z \lesssim 1$. The color of red galaxies at a given rest-frame magnitude becomes bluer with increasing redshift. The quantitative size of this change is consistent with passive aging of ancient stellar populations to the present day.

Using this empirically-motivated definition of early-type galaxies, we estimate the rest-frame B -band luminosity function and luminosity density of red-sequence galaxies in the interval $0 < z \leq 1.1$. There may be some contribution from dusty star-forming galaxies at the highest redshifts, making our results upper limits. Nevertheless, we find mild evolution of the rest-frame B -band luminosity density between $0 < z \leq 1.1$. Ancient stellar populations would fade by a factor of two to three in this time interval; therefore, this mild evolution betrays an increase in the stellar mass on the red sequence since $z \sim 1$ by at least a factor of two. This evolution is consistent qualitatively and quantitatively with the evolution expected from the hierarchical build-up of stellar mass via galaxy mergers in a Λ CDM Universe. The largest source of error is large-scale structure, implying that considerably larger surveys are necessary to further refine this result.

Finally, we explore the evolution of the red, blue and gap population on the color-magnitude plane. We find that a scenario in which SF is stopped (for an as-yet-unspecified reason) in 5–10% of the blue galaxy population per Gyr reproduces the relative numbers of red, blue and gap galaxies. We argue also, based on the luminosity functions and morphologies of red galaxies in the local and distant Universe, that galaxy merging plays an important role. In particular, at least some of the the most luminous red galaxies must be formed in galaxy mergers which are either very dusty or take place between gas-poor progenitors. Disentangling further the processes which drive the evolution of the red galaxy population at $z \lesssim 1$ will indeed present a fascinating observational challenge over the next few years.

E. F. B. was supported by the European Research Training Network *Spectroscopic and Imaging Surveys for Cosmology*. C. W. was supported by the PPARC rolling grant in Observational Cosmology at University of Oxford and by the DFG-SFB 439. We wish to thank Carlton Baugh for providing blind predictions of the Cole et al. (2000) GALFORM semi-analytic model, and thank David Anderson, Marco Barden, Stephane Charlot, David Hogg, Guinevere Kauffmann, Alvio Renzini, and Scott Trager for useful discussions and suggestions. Jim Pee-

bles is thanked for his comments on an earlier version of the manuscript. This publication makes use of the *Sloan Digital Sky Survey* (SDSS). Funding for the creation and distribution of the SDSS Archive has been provided by the Alfred P. Sloan Foundation, the Participating Institutions, the National Aeronautics and Space Administration, the National Science Foundation, the US Department of Energy, the Japanese Monbukagakusho, and the Max Planck Society. The SDSS Web site is <http://www.sdss.org/>. The SDSS Participating Institutions are the University of Chicago, Fermilab, the Institute for Advanced Study, the Japan Participation Group, the Johns Hopkins University, the Max Planck Institut für Astronomie, the Max Planck Institut für Astrophysik, New Mexico State University, Princeton University, the United States Naval Observatory, and the University of Washington. This publication made use of NASA's Astrophysics Data System Bibliographic Services.

REFERENCES

- Aragon-Salamanca, A., Baugh, C. M., & Kauffmann, G. 1998, MNRAS, 297, 427
 Baade, D., et al. 1998, The Messenger, 93, 13
 Baade, D., et al. 1999, The Messenger, 95, 15
 Barnes, J. E. 1992, ApJ, 393, 484
 Barnes, J. E., & Hernquist, L. 1996, ApJ, 471, 115
 Barton, E. J., Geller, M. J., & Kenyon, S. J. 2000, ApJ, 530, 660
 Baugh, C. M., Cole, S., & Frenk, C. S. 1996, MNRAS, 283, 1361
 Bell, E. F., & de Jong, R. S. 2000, MNRAS, 312, 497
 Bell, E. F., McIntosh, D. H., Katz, N., & Weinberg, M. D. 2003, submitted to ApJ (astro-ph/0302543)
 Bernardi, M., et al. 1998, ApJ, 508, L143
 Bernardi, M., et al. 2003, AJ, in press (astro-ph/0301629)
 Bertin, E., & Arnouts, S. 1996, A&AS, 117, 393
 Blanton, M. R., et al. 2001, ApJ, 121, 2358
 Blanton, M. R., et al. 2003a, submitted to ApJ (astro-ph/0209479)
 Blanton, M. R., et al. 2003b, submitted to ApJ (astro-ph/0210215)
 Bower, R. G., Kodama, T., & Terlevich, A. 1998, MNRAS, 299, 1193
 Bower, R. G., Lucey, J. R., & Ellis, R. S. 1992, MNRAS, 254, 601
 Butcher, H., & Oemler, Jr., A. 1984, ApJ, 285, 426
 Calzetti, D., Armus, L., Bohlin, R. C., Kinney, A. L., Koornneef, J., & Storchi-Bergmann, T. 2000, ApJ, 533, 682
 Charlot, S., Worthey, G., & Bressan, A. 1996, ApJ, 457, 625
 Chen, H.-W., et al. 2003, ApJ, in press (astro-ph/0212147)
 Cimatti, A., et al. 2002, A&A, 381, L68
 Cole, S., Lacey, C., Baugh, C. M., & Frenk, C. S. 2000, MNRAS, 319, 168
 Couch, W. J., Barger, A. J., Smail, I., Ellis, R. S., & Sharples, R. M. 1998, ApJ, 497, 188
 Cowie, L. L., Songaila, A., Hu, E. M., Cohen, J. G. 1996, AJ, 112, 839
 Daddi, E., et al. 2002, A&A, 384, L1
 Dressler, A. 1980, ApJ, 236, 351
 Dressler, A., et al. 1997, ApJ, 490, 577
 Efstathiou, G., et al. 2002, MNRAS, 330, L29
 Eggen, O. J., Lynden-Bell, D., & Sandage, A. R. 1962, ApJ, 136, 748
 Felten, J. E. 1977, AJ, 82, 861
 Fioc, M., & Rocca-Volmerange, B. 1997, A&A, 326, 950
 Firth, A. E., et al. 2002, MNRAS, 332, 617
 Freedman, W. L., et al. 2001, ApJ, 553, 47
 Guzman, R., Lucey, J. R., Carter, D., Terlevich, R. J. 1992, MNRAS, 257, 187
 Hogg, D. W., et al. 2002, AJ, 124, 646
 Hogg, D. W., et al. 2003, ApJ, 585, L5
 Im, M., Griffiths, R. E., Ratnatunga, K. U., & Sarajedini, V. L. 1996, ApJ, 461, L79
 Im, M., et al. 2002, ApJ, 571, 1361
 Jansen, R., Franx, M., Fabricant, D., & Caldwell, N. 2000, ApJS, 126, 271
 Kauffmann, G., & Charlot, S. 1998, MNRAS, 297, L23
 Kauffmann, G., Charlot, S., & White, S. D. M. 1996, MNRAS, 283, L117
 Kauffmann, G., Colberg, J. M., Diaferio, A., & White, S. D. M. 1999, MNRAS, 303, 188
 Kelson, D. D., Illingworth, G. D., Franx, M., & van Dokkum, P. G. 2001, ApJ, 552, L17
 Khochfar, S., & Burkert, A. 2003, submitted to ApJL
 Kinney, A. L., Calzetti, D., Bohlin, R. C., McQuade, K., Storchi-Bergmann, T., & Schmitt, H. R. 1996, ApJ, 467, 38
 Kochanek, C. S., et al. 2000, ApJ, 543, 131
 Kochanek, C. S., et al. 2001, ApJ, 560, 566
 Kodama, T., & Arimoto, N. 1997, A&A, 320, 41

- Kodama, T., Bower, R. G., & Bell, E. F. 1999, MNRAS, 306, 561
 Kron, R. G. 1980, ApJS, 43, 305
 Kuntschner, H. 2000, MNRAS, 315, 184
 Larson, R. B. 1975, MNRAS, 173, 671
 Lilly, S. J., Tresse, L., Hammer, F., Crampton, D., & Le Fèvre, O. 1995, ApJ, 455, 108
 Lin, H., et al. 1999, ApJ, 518, 533
 Madgwick, D. S., et al. 2002, MNRAS, 333, 133
 McIntosh, D. H., Rix, H.-W., & Caldwell, N., 2003, submitted to ApJ(astro-ph/0212427)
 Menanteau, F., Ellis, R. S., Abraham, R. G., Barger, A. J., Cowie, L. L. 1999, MNRAS, 309, 208
 Moustakas, L. A., & Somerville, R. S. 2002, ApJ, 577, 1
 Nulsen, P. E. J., & Fabian, A. C. 1997, MNRAS, 291, 425
 Peletier, R. F., Davies, R. L., Illingworth, G. D., Davis, L. E., & Cawson, M. 1990, AJ, 100, 1091
 Pozzetti, L., et al. 2003, A&A, in press (astro-ph/0302599)
 Pryke, C., Halverson, N. W., Leitch, E. M., Kovac, J., Carlstrom, J. E., Holzappel, W. L., & Dragovan, M. 2002, ApJ, 568, 46
 Röser, H.-J., & Meisenheimer, K. A&A, 252, 458
 Rusin, D., et al. 2003, ApJ, in press (astro-ph/0211229)
 Salpeter, E. E. 1955, ApJ, 121, 161
 Sandage, A., & Visvanathan, N. 1978, ApJ, 225, 742
 Sandage, A., Tammann, G. A., & Yahil, A. 1979, ApJ, 232, 352
 Schade, D., et al. 1999, ApJ, 525, 31
 Schechter, P. 1976, ApJ, 203, 297
 Schlegel, D. J., Finkbeiner, D. P., & Davis, M. 1998, ApJ, 500, 525
 Schweizer, F., & Seitzer, P. 1992, AJ, 104, 1039
 Skrutskie, M. F., et al. 1997, in 'The Impact of Large Scale Near-IR Sky Surveys', eds. F. Garzon et al., p 25. (Dordrecht: Kluwer Academic Publishing Company)
 Somerville, R. S., & Primack, J. R. 1999, MNRAS, 310, 1087
 Spergel, D. N., et al. 2003, submitted to ApJ (astro-ph/0302209)
 Stoughton, C., et al. 2002, AJ, 123, 485
 Strateva, I., et al. 2001, AJ, 122, 1861
 Terlevich, A. I., Caldwell, N., & Bower, R. G. 2001, MNRAS, 326, 1547
 Toomre, A., & Toomre, J. 1972, ApJ, 178, 623
 Totani, T., & Yoshii, Y. 1998, ApJ, 501, L177
 Trager, S. C., Faber, S. M., Worthey, G., & González, J. J. 2000, AJ, 120, 165
 Treu, T., Stiavelli, M., Casertano, S., Möller, P., & Bertin, G. 2002, ApJ, 564, L13
 Tully, R. B., Pierce, M. J., Huang, J.-S., Saunders, W., Verheijen, M. A. W., & Witchalls, P. L. 1998, AJ, 115, 2264
 van de Ven, G., van Dokkum, P. G., & Franx, M. 2003, submitted to MNRAS(astro-ph/0211566)
 van Dokkum, P. G., & Franx, M. 2001, ApJ, 553, 90
 van Dokkum, P. G., & Franx, M., Fabricant, D., Illingworth, G. D., & Kelson, D. D. 2000, ApJ, 541, 95
 van Dokkum, P. G., Stanford, S. A., Holden, B. P., Eisenhardt, P. R., Dickinson, M., & Elston, R. 2001, ApJ, 552, L101
 van Dokkum, P. G., et al. 2003, ApJL, in press (astro-ph/0303166)
 Vazdekis, A., Kuntschner, H., Davies, R. L., Arimoto, N., Nakamura, O., & Peletier, R. 2001, ApJ, 551, L127
 White, S. D. M., & Frenk, C. S. 1991, ApJ, 379, 52
 Wolf, C., Meisenheimer, K., Röser, H.-J. 2001, A&A, 365, 660 (W01)
 Wolf, C., et al. 2001b, A&A, 365, 681
 Wolf, C., Meisenheimer, K., Rix, H.-W., Borch, A., Dye, S., & Kleinheinrich, M. 2003, A&A, in press (W03; astro-ph/0208345)
 Yan, L., & Thompson, D. 2003, astro-ph/0212153
 Ziegler, B. L., Bower, R. G., Smail, I., Davies, R. L., Lee, D. 2001, MNRAS, 325, 1571

APPENDIX

RED-SEQUENCE GALAXIES IN THE LOCAL UNIVERSE

Because of its homogeneity and color information, the SDSS Early Data Release (EDR; Stoughton et al. 2002) offers an ideal comparison sample to COMBO-17 at redshift zero. In order to compare as fairly as possible with COMBO-17, we choose to synthesize U , B , and V magnitudes from SDSS ugr data, using the UBV bandpasses that were used to construct COMBO-17 rest-frame magnitudes. We adopt the transformations:

$$U - V = -0.713 + 0.826(u - r); \sigma \sim 0.023, \quad (\text{A1})$$

$$g - B = -0.155 - 0.370(g - r); \sigma \sim 0.012, \quad (\text{A2})$$

$$g - V = -0.010 + 0.609(g - r); \sigma \sim 0.006, \quad (\text{A3})$$

which were derived from the single stellar populations from the PÉGASE stellar population synthesis model, and are valid

for stellar populations between $1/200$ and $5 \times$ solar metallicity, and ages between 50 Myr and 20 Gyr. These transformations are dominated by the systematic zero point uncertainties (in absolute terms) of the SDSS and Johnson photometric system, and by limitations of the SDSS Petrosian magnitude. These uncertainties are likely $\lesssim 0.1$ mag in terms of color, although absolute calibration of u or U -band data is always challenging. SDSS EDR galaxies were chosen to have measured redshifts and a reddening-corrected Petrosian magnitude in r between $13 \leq r \leq 16$, yielding a total sample of 3069 galaxies. The Petrosian magnitude of concentrated (i.e. early-type) galaxies is corrected by -0.15 mag to crudely account for the well-known shortfall of Petrosian magnitudes for centrally-concentrated galaxies (e.g., Blanton et al. 2003b).

We show the distribution of synthesized $U - V$ color against M_V in the left-hand panel of Fig. A6. There is a well-defined CMR, which has scatter ~ 0.2 mag; this large scatter is expected, as SDSS $u - r$ magnitudes have typical uncertainties ~ 0.15 mag, after observational error and evolution and K -correction errors are accounted for. The intercept of the CMR is consistent with the intercept of the Abell 754 galaxy cluster (McIntosh, Rix, & Caldwell 2003) and the Nearby Field Galaxy Survey (Jansen et al. 2000) morphologically-classified early-type galaxy CMR to within 0.1 mag. This kind of offset is not unexpected given the difficulty of calibrating absolute photometry to better than 10%. The blue peak is relatively small in these data, because the data are apparent magnitude limited in the r -band, which increases the dominance of bright red galaxies compared to their fainter, blue star-forming counterparts.

Following Bell et al. (2003), we construct a rest-frame B -band luminosity function of red-sequence galaxies (redder than the dashed line in Fig. A6) using the V/V_{\max} formalism. It should be noted that galaxy selection for inclusion in this luminosity function is unbiased by any zero-point uncertainty in calibration, as this criterion is applied relative to the ridge-line of the CMR, which is measured using the same data. In order to constrain the effects of magnitude error (from photometric redshift error) on the luminosity function (as discussed by Chen et al. 2003), we convolve our B -band luminosities with a random 0.4 mag error, which simulates a $\delta z \sim 0.03$ at $z \sim 0.25$ (our lowest redshift bin). We also constrain the faint-end slope $\alpha = -0.9$, to match with the COMBO-17 luminosity function determinations. The Schechter function fit parameters are $\phi^* = 7.2 \pm 0.6 \times 10^{-3} h^3 \text{Mpc}^{-3} \text{mag}^{-1}$, $M_B^* - 5 \log_{10} h = -19.63 \pm 0.08$, $\alpha = -0.9$, and $j_B = 7.5 \pm 0.2 \times 10^7 L_{\odot} h \text{Mpc}^{-3}$ (random errors only). The luminosity function calculated in this way is shown by the solid black circles and solid line in the right-hand panel of Fig. A6. For reference, a Schechter function fit to the unconvolved (i.e. real) B -band synthesized luminosity function is shown by the dotted line. The M^* of this fit is ~ 0.25 mag fainter than the convolved fit (with corresponding increase of ϕ^* to compensate); this modest offset is the maximum bias that we expect in the Schechter fit parameters because of our use of 17-passband derived photometric redshifts. This is in agreement with Chen et al. (2003), who show that we would expect only a modest bias towards brighter M^* because of our relatively small photometric redshift uncertainty. The uncertainty in luminosity density is roughly 10% in a systematic sense; this error is dominated by uncertainties in absolute magnitude calibration and in correcting the luminosity function normalization to the observed all-sky $|b| \geq 30^\circ$ density of $10 < K < 13.5$ galaxies.

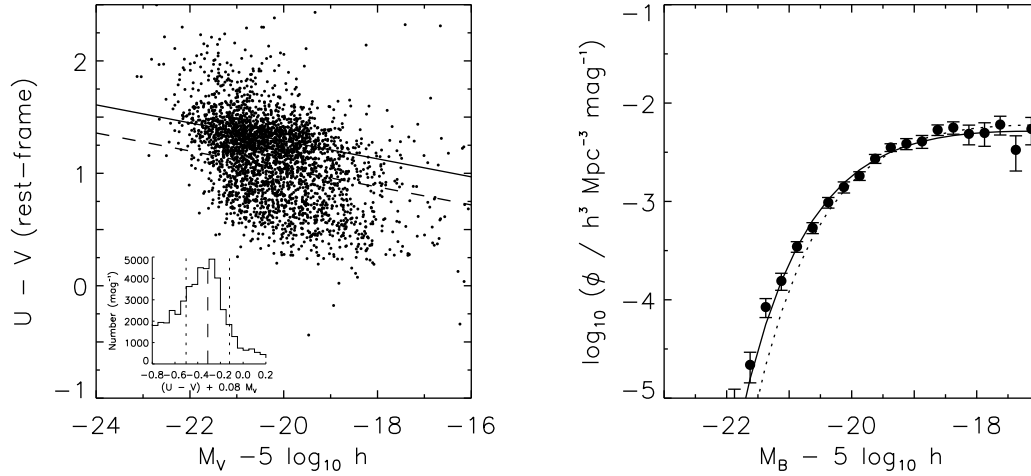


FIG. A6.— Rest-frame synthesized $U-V$ colors and B -band luminosity function of SDSS EDR galaxies. The left-hand panel shows the synthesized $U-V$ vs. M_V color-magnitude diagram for SDSS EDR galaxies selected to have $13 \leq r \leq 16$. The solid and dotted lines show the best-fit CMR and the Butcher-Oemler-style cutoff adopted in this paper, assuming a slope of -0.08 (following Bower, Lucey, & Ellis 1992; Terlevich, Caldwell, & Bower 2001). The inset panel shows the color distribution of these galaxies, with the slope of the CMR taken out. The right-hand panel shows the rest-frame B -band luminosity function of the red-sequence galaxies, assuming a 0.4 mag magnitude error caused by photometric redshift uncertainty. The solid circles with error bars show the V/V_{\max} estimates, and the solid line a Schechter fit to these estimates. The dotted line shows the Schechter fit to the B -band luminosity function without the additional 0.4 mag scatter.

For more discussion of the selection, photometric parameters, V/V_{\max} luminosity function estimation, and uncertainties, see Bell et al. (2003).